# List of supplementary files for "Biotite/melt trace-element, lithium, and F-OH partitioning in silicate magmas" Beard et al., 2026, Journal of Petrology

## Electronic appendix A (.kml):

A waypoint file for field localities for the Canary Islands pyroclastic rock samples

## Electronic appendix B (.xlsx):

A spreadsheet containing (1) Compositions of starting materials for the IHPV experiments; (2) Experiment run conditions; (3) Electron microprobe (EPMA) major-element data for experiment and Canary Islands biotite; (4) EPMA major-element data for experiment and Canary Islands glass; (5) EPMA reference material measurements, including comparison to values retrieved from the GeoReM database (Jochum *et al.* 2005; compiled values from Govindaraju 1994); (6) Laser ablation ICP-MS measurements of Canary Islands biotite and glass; (7) Laser ablation measurements of experimental run products; (8) Laser ablation analyses of reference materials compiled across several measurement sessions, including comparison to compiled values retrieved from the GeoReM database (Jochum *et al.* 2005, 2011, 2016; Smith 1995; John Stix 2015 compilation) (9) Deconvolved analyses of biotite and glass via LA-ICP-MS; (10) Nernst partition coefficients (D values) for major- and trace-elements as determined from EPMA and LA-ICP-MS analyses; (11) and finally a spreadsheet for assigning biotite major-element ions to lattice sites following Li *et al.* (2020) modified after Zhang *et al.* (2022), for calculating silicate melt water speciation following Behrens (2020), and subsequently melt $XF$ and $XOH$ values, melt NBO/T following Mills (1993), and for determining modelled F-OH and Cl-OH exchange coefficients following Zhang *et al.* (2022), and F-OH exchange, $^{XII}$A-site lattice strain parameters, $D$ values for Na, K, Rb, Cs, Li and Nb using our new empirical partitioning models.

## Electronic appendix C (.zip):

A folder containing MATLAB scripts for reduction of laser-ablation trace-element measurements from both unmixed and mixed analyses of silicate glass and biotite. These codes require installation of the MATLAB machine learning and curve fitting toolbox. All input files required by these codes containing EPMA and LA-ICP-MS data are included in this folder. The codes generate a series of robust regression diagrams of biotite or glass proportion, constrained by the Mg/Al and Na/Al ratio respectively, a

diagram showing the determined biotite and glass trace-element concentrations with their associated uncertainty and finally a diagram of trace-element $D$ values.

## Electronic appendix D (.zip):

A folder containing (1) a subfolder of Onuma diagrams (Onuma *et al.*, 1968) for the biotite $^{XII}$A-site per experiment showing 1σuncertainty on 1+ partition coefficients and a 1σerror envelope on the lattice strain curve. The folder also contains histograms for fitted lattice strain parameters as determined via bootrapping; (2) multiple regression reports for empirical element partitioning models as generated using the NCSS software.

# Supplementary figures for "Biotite/melt trace-element, lithium, and F-OH partitioning in silicate magmas" Beard et al., 2026, Journal of Petrology

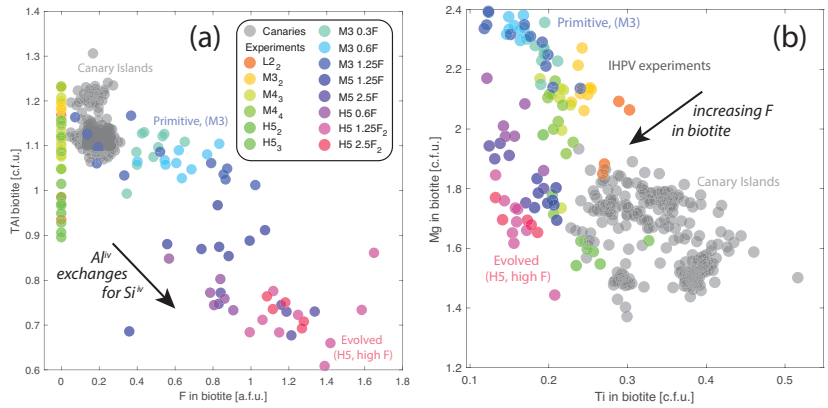



**Figure S1** Major-element compositions of biotite from the Canary Islands pyroclastic rocks, compared with those produced in the internally heated pressure vessel experiments. (a) Tetrahedral Al vs. F content, (b) Mg vs. Ti content. Arrow shows compositional offset in biotite for the same experiment starting composition when fluorine is added. Ionic site assignments are calculated based on a total cation charge of 22 per formula unit.

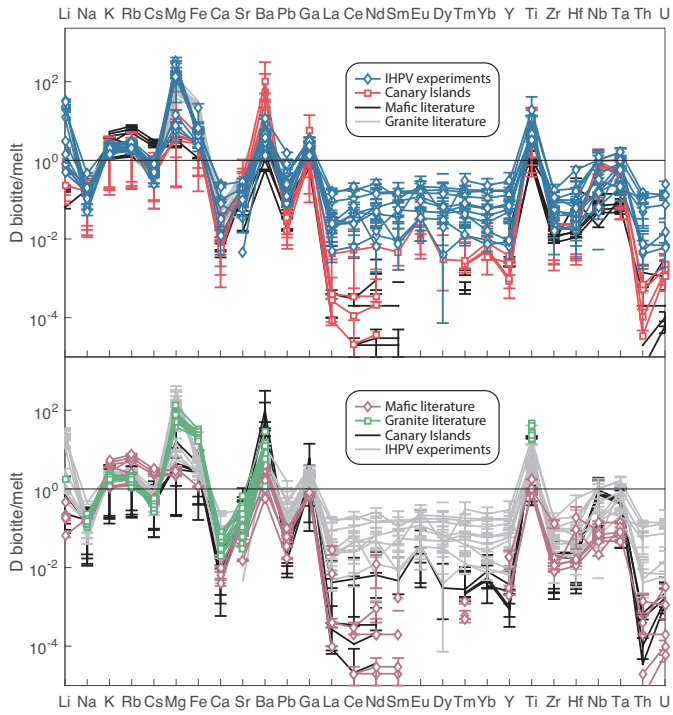



**Figure S2** Biotite/melt element partition coefficients for experiments and Canary Islands pyroclastic rocks, including partition coefficients for the REE. Shown for comparison are published experimental partition coefficients for mafic compositions from Adam *et al.* (1993); LaTourrette *et al.* (1995); Schmidt *et al.* (1999); Green *et al.* (2000); Adam & Green (2006), and from granitic compositions from Icenhower & London (1995, 1997). Note how $D_{\mathrm{La}}$ is slightly higher than $D_{\mathrm{Ce}}$ in case of the Canary Island rocks and mafic experiments from Adam & Green (2006). Note that $D_{\mathrm{REE}}$ for the IHPV experiments from this study are unreliable, because the REE concentration in the biotite is at or below the detection limit of our LA-ICP-MS setup.

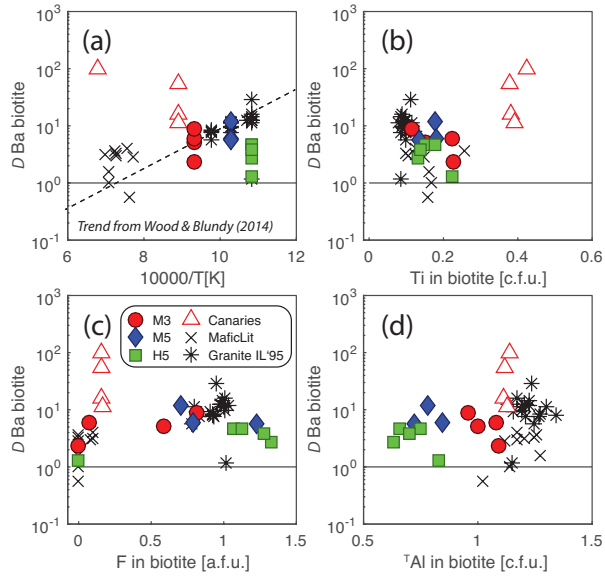



**Figure S3** Barium partitioning vs. inverse temperature and compositional parameters for biotite. (a) follows Wood & Blundy (2014, literature data), where our experimental results for the M3 and M5 composition are consistent with trends defined by published $D_{Ba}$ values (citation in prev. figs), with our Canaries samples returning consistently higher values for $D_{Ba}$ and experiments on the H5 composition consistently lower. (b) shows that the elevated $D_{Ba}$ values of the Canaries biotite are correlated with their high Ti contents. (c) shows a poor correlation between F in biotite and $D_{Ba}$, and (d) shows a weak positive correlation between tetrahedral Al and $D_{Ba}$. Literature data sources as listed in Fig. 5.

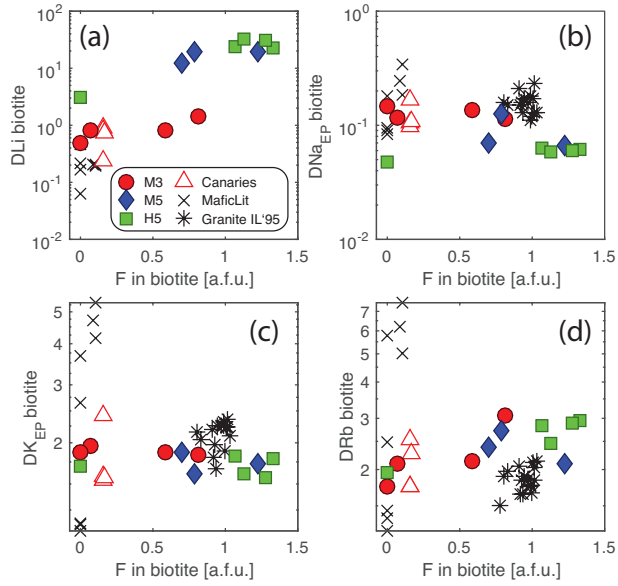



**Figure S4** Partitioning of 1+ elements vs. fluorine content of the biotite, calculated on the basis of 22 charges per formula unit. Mafic literature data sources as listed in Fig. 5. IL'95 is Icenhower & London (1995).

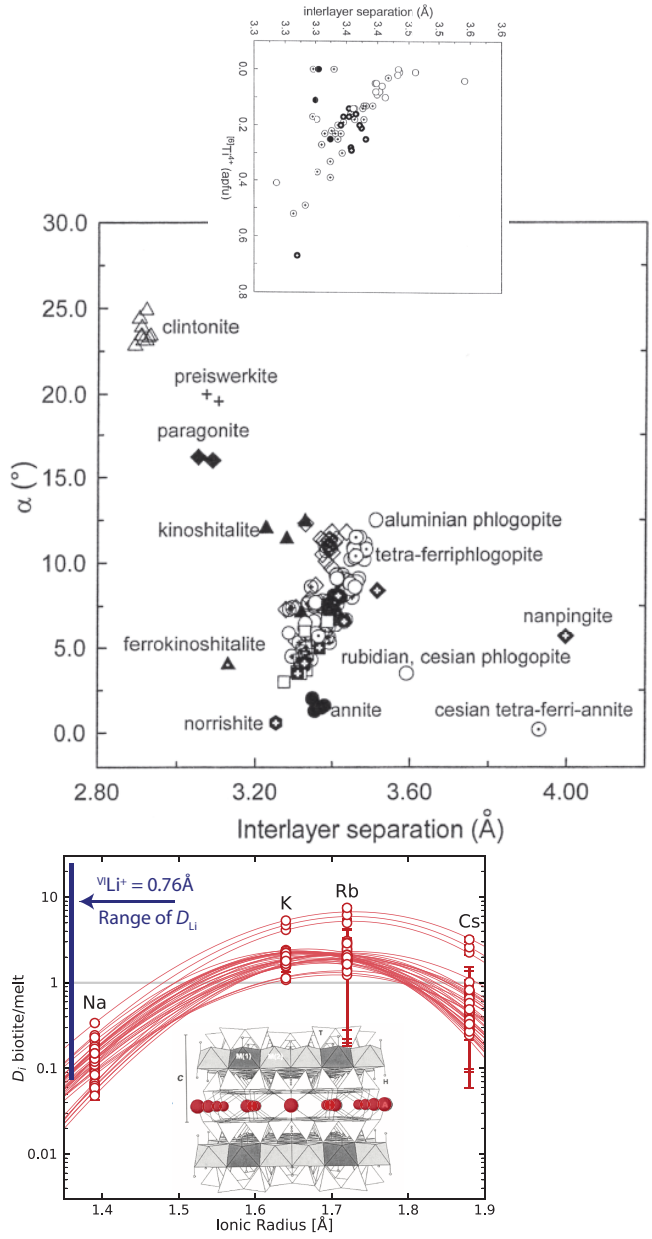



**Figure S5** Onuma diagram for the partitioning of 1+ cations between the mica interlayer site and silicate melt. Interlayer separation diagrams from Brigatti & Guggenheim (2002) for comparison, where the radius scale is aligned to half of the interlayer separation value.

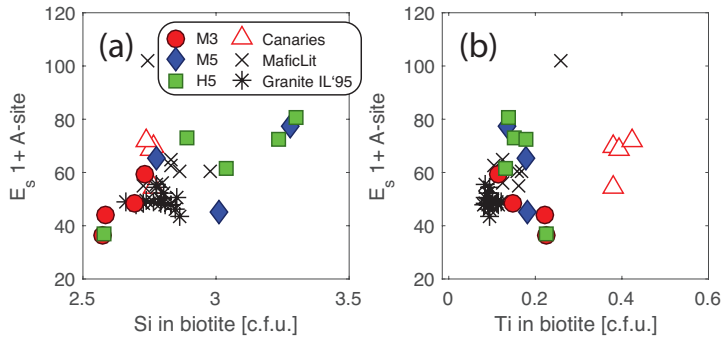



**Figure S6** Young's modulus for 1+ ions in the A-site of biotite vs. compositional parameters.

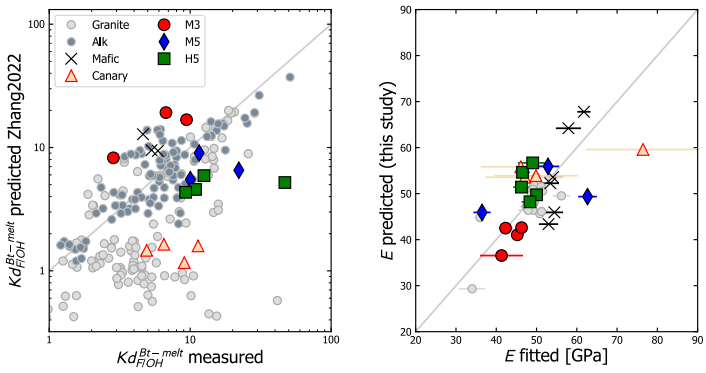



**Figure S7** Measured vs. predicted diagrams for (left) Kd F-OH for the empirical model of Zhang *et al.* (2022), which broadly reproduces our experimental data set, but systematically underpredicts $Kd$ values for the peraluminous granite experiments of Icenhower & London (1995) and our Canary Islands natural mineral-melt pairs. The right panel shows performance of our model for the E parameter of the lattice strain model for 1+ cations at the biotite XII-coordinated A-site.

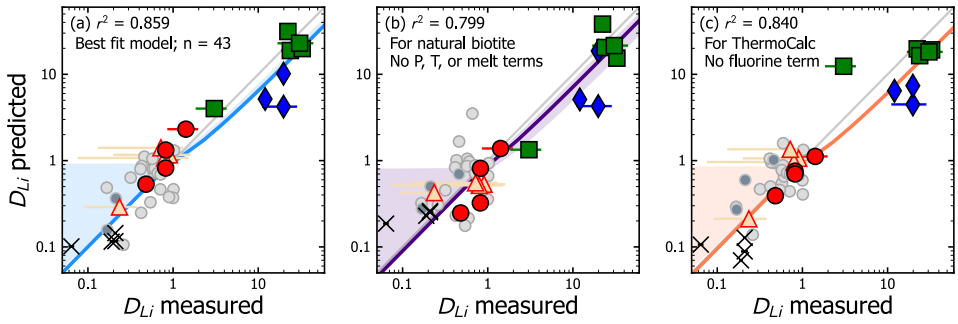



**Figure S8** Measured vs. predicted diagrams for three contrasting empirical models for lithium partitioning between biotite and melt. The gray diagonal lines show 1:1 relationships between measured and predicted $D_{\mathrm{Li}}$ values. Coloured regression lines are robust fits to the partitioning data with uncertainty envelopes shown at the $1\sigma$ level.